



## Technical note

## Arbitrary waveform constant current stimulator for long-term wearable applications

Paul P. Breen<sup>a,b,\*</sup>, Jorge M. Serrador<sup>c,d,e</sup>, Gaetano D. Gargiulo<sup>a,b</sup><sup>a</sup>The MARCS Institute for Brain, Behaviour and Development, Western Sydney University, Penrith, NSW, Australia<sup>b</sup>Translational Health Research Institute, Western Sydney University, Penrith, NSW, Australia<sup>c</sup>Department of Pharmacology, Physiology & Neuroscience, Rutgers Biomedical and Health Sciences, Newark, NJ, USA<sup>d</sup>National University of Ireland Galway, Galway, Ireland<sup>e</sup>Department of Veteran Affairs, NJ Health Care System, War Related Illness & Injury Study Center, East Orange, NJ, USA

## ARTICLE INFO

## Article history:

Received 12 June 2018

Revised 29 January 2019

Accepted 3 April 2019

## Keywords:

Neural facilitation

Constant current stimulation

Stochastic resonance

Neural facilitation

## ABSTRACT

Subsensory electrical noise stimulation has been shown to improve sensory perception in humans. However, the majority of this work has been limited to the laboratory due to unavailability of portable body-worn stimulators. In this paper, we present a robust and reliable stimulator, engineered for wearable applications and designed to extend modulation of human sensory perception outside the physiology laboratory.

The stimulator provides an arbitrary waveform constant current stimulation, offering continuous current stimulation up to  $\pm 5$  mA with a voltage compliance of  $\pm 25$  V (expandable up to 70 V). A graphical user interface allows setting of stimulus parameters within fixed ranges via a USB connected computer. The interface is very simple using a single power switch and a single multi-coloured LED for device feedback. The applied stimulus voltage and current are continually monitored and used to detect short circuit, high impedance conditions. These conditions, and other errors e.g. low battery state, put the device in a safe state with the user disconnected via a relay. All captured data, including accelerometer data, is logged to a removable SD card. Powered by an interchangeable, Li-Ion battery pack >4 h stimulation is achievable. The full circuit, system software and bench tests performed are presented.

© 2019 IPEM. Published by Elsevier Ltd. All rights reserved.

## 1. Introduction

Neural function may be diminished through injury or disease and is seen as a normal decline associated with ageing [1,2]. Among other potential impairments, loss of somatosensory function can lead to a reduced touch perception, protective sensation and balance [3,4]. It can contribute to the development of foot ulceration or increase risk of falls and fractures [5,6]. Currently, there is little that can be done to restore this function once it is lost.

In recent years, a substantial amount of work has been performed to address sensory deficits through the external application of a noise stimulus [7]. Termed stochastic resonance by many authors the process could be more generally termed *stochastic facilitation*. Practically, stochastic facilitation is observed within a

specific neural system when the function of that neural system is arguably improved in the presence of some stochastic, biologically relevant noise [7]. This intervention has taken many forms including mechanical and electrical stimulation, and has been shown to improve a variety of somatosensory functions in both healthy and patient cohorts [8–13]. Typically, but not exclusively, the applied stimulus is a subsensory constant Gaussian white or pink noise, delivered transcutaneously via surface electrodes.

Indeed, while many of these experiments have shown good efficacy and hold some promise as a future electroceutical there is very little evidence of efficacy beyond lab based experiments or short-term studies. Of greatest concern is that little is known about the medium to long-term side-effects of any of these propose treatments. Electrical stimulation at higher current levels can result in thermal damage to the skin, burns and/or general discomfort [14–16]. While none of these issues have been reported with subsensory stimulation, nothing is known about medium or long-term effects on comfort, skin integrity or indeed neural responses. We would suggest that the lack of an appropriate means of delivering this treatment in a safe, compact and non-intrusive form is a primary limiting factor for researchers in this area.

\* Corresponding author at: The MARCS Institute for Brain, Behaviour and Development, Western Sydney University, Locked Bag 1797, Penrith, NSW 2751, Australia.

E-mail addresses: [p.breen@westernsydney.edu.au](mailto:p.breen@westernsydney.edu.au) (P.P. Breen), [serradjo@njms.rutgers.edu](mailto:serradjo@njms.rutgers.edu) (J.M. Serrador), [g.gargiulo@westernsydney.edu.au](mailto:g.gargiulo@westernsydney.edu.au) (G.D. Gargiulo).

To address this bottleneck, we have developed a novel constant current stimulator platform that we believe is suitable to deliver the previously explored electroceutical treatments in medium to long-term studies of efficacy. The requirements of this stimulator differ in many respects to those presently available on the market. To begin with, it is a wearable solution whereas many of the previous experiments relied on benchtop stimulator devices. Second, it requires the delivery of an arbitrary constant current stimulus, a more difficult stimulus to deliver than a traditional, regular, pulsatile or sinusoidal stimulus (e.g., [17]), and one that inherently increases the power requirements of the device. A small number of portable stimulators have been reported that can provide an arbitrary current output. The RehaMovePro is mobile and can create a custom waveform but has too large a current resolution (0.5 mA) for this application [18]. Another device by Yamamoto has a limited voltage compliance ( $\pm 10$  V) and is not capable of collecting data on the stimulus applied over time [19].

Device specifications are drawn from experience in previous work [12,13,20]. However, the platform stimulator is capable of being reprogrammed to deliver any desired stimulus output within its frequency and amplitude limits. The stimulus required is largely low frequency, with substantial 10 dB/decade attenuation with frequency (1/f noise). Over long term use, tracking current and impedance is important so an anti-aliasing filter of  $\sim 300$  Hz is required. Voltage compliance of  $\pm 25$  V and a max current of  $\pm 2.5$  mA is necessary. Power requirements are significant as the device may operate throughout the day. Finally, as with any such device, user-friendly, safe and appropriate stimulus delivery is paramount.

We present this device in its entirety and include details on software, circuitry, enclosures, specifications of components and bench test results. While there is scope for improvement in the design and implementation, it should serve as a starting point for many in the development of stochastic facilitation based treatments for somatosensory impairments.

## 2. Methods

The aim of this work was to provide a robust and reliable stimulator system that provides arbitrary waveform constant current stimulation for human applications of neural facilitation. The system may be subdivided into five primary functional blocks – digital, stimulator, sensing, user interface and power. The block diagram of Fig. 1. gives an overview of how these subsystems interact, while the following sections and supplementary material provide greater detail of each individual subsection. Please note, standard decoupling capacitors were used throughout, but are not shown in the circuit diagrams that follow.

### 2.1. Power block

#### 2.1.1. Digital supply

As the microcontroller operates at 3.3 V, analogue inputs and outputs are confined within the 0–3.3 V single ended voltage dynamic range. However, bidirectional current stimulation requires a bipolar voltage dynamic, thus both control and acquired signals need to be offset and spanned. The necessary offset and spans for the driving stimulus and read-back signal manipulation are implemented using low noise low power precision operational amplifiers OPA244 [21].

The microcontroller is powered by a single 3.7 V li-ion cell. As it was intended to create a 1 mA/V voltage-to-current converter with an absolute maximum  $\pm 5$  mA output, a  $\pm 5$  V supply was required and is derived from the high-voltage supply. Although this is not an entirely efficient solution, it does eliminate the alternative need for an additional cell on the microcontroller side. It further means

that the entire analogue circuitry is powered from a single step-up circuit. We implemented the  $\pm 5$  V supply using 35 V compatible versions of the well-known LM7805 and LM7905. In practice the absolute maximum current output was not used, but instead limited to  $\pm 2.5$  mA.

#### 2.1.2. Stimulator supply

The stimulator requires a high voltage power supply which is implemented using the LM2587 flyback regulator from Texas Instruments [22], capable of providing an output of up to 65 V from an input just over 4 V. This circuit is powered by a 11.1 V source implemented with a series of three 3.7 V li-ion cells. The high-voltage supply was limited to 50 V, and split to  $\pm 25$  V by a compensated passive voltage divider (Fig. 2B). This technique proved successful to power biomedical amplifiers, including when used in driven right leg circuitry.

As a result, at maximum output ( $\pm 2.5$  mA), this stimulator can withstand a total body impedance of 10 k $\Omega$ . These values have been selected based on prior experimental experience and to avoid forced stimulation in abnormal conditions. These compliance level are appropriate considering an expected minimum skin impedance of 5 k $\Omega$ , balanced with the fact that prolonged forced stimulation when contact impedance is high can result in thermal damage to the skin, burns and/or general discomfort [14–16].

Sensory thresholds are often used as a guide to the level of stimulus to apply. The output current range must be sufficient to generate perceptible stimuli despite being subthreshold in practice. Sensory thresholds increase with age so we based the output current range on our previous experiments, and those conducted by other authors, that included experiments with older adults [9,12,23–25]. As electrode impedance may increase over time, and the device is intended for continuous use during waking hours, a large voltage compliance is necessary. It should be noted that electrode type/size, impedance and site of application may further affect sensory threshold. We believe the current and voltage ranges are sufficient to accommodate long-term evaluations of previously completed laboratory based experiments.

### 2.2. Stimulator block

#### 2.2.1. Offset and span

In order to interface the 3.3 V microcontroller with the much higher voltages of the stimulator circuitry ( $\pm 25$  V), three offset-span circuits are implemented. The offset-span circuits all use a common voltage bias obtained by a voltage follower (Fig. 2A, U1). This value is set during calibration using a 25-turn trimmer at its input.

#### 2.2.2. Constant current generator

The core of the arbitrary waveform constant current stimulator circuit (Fig. 2B) is a modified Howland pump circuit designed around the ADA4700-1 high voltage, precision operational amplifier by Analogue Devices [26,27]. This chip was selected because of its high voltage compliance (up to 100 V), high current drive (up to 30 mA) and as it is recommended by the manufacturer for current sourcing applications.

To ensure that bipolar current may be generated and the user is not a floating load, the current source must have a corresponding current sink, i.e. one of the acts as source and the other as sink. To achieve this, two ADA4700-1 chips (U3 & U4) were arranged to form a bidirectional current source/sink circuit across the stimulation electrodes (E1 & E2) drawing power from a high-voltage compliant power supply. One ADA4700-1 is employed as the modified Howland pump (U3), and the second as a current sink (U4). This bootstrapped current sink receives half of the 50 V stimulator supply voltage as an input, i.e. the stimulator system ground.

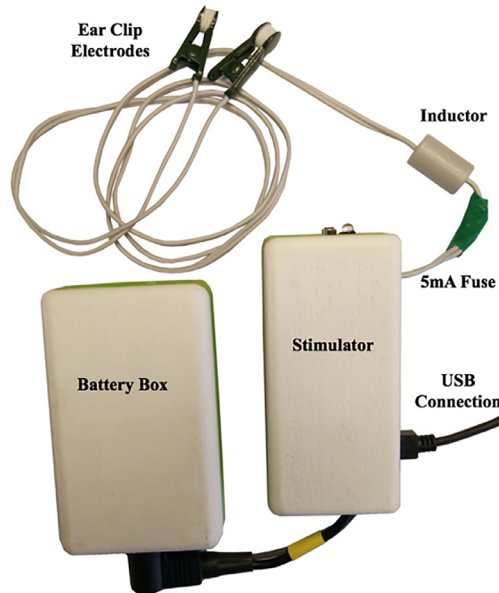
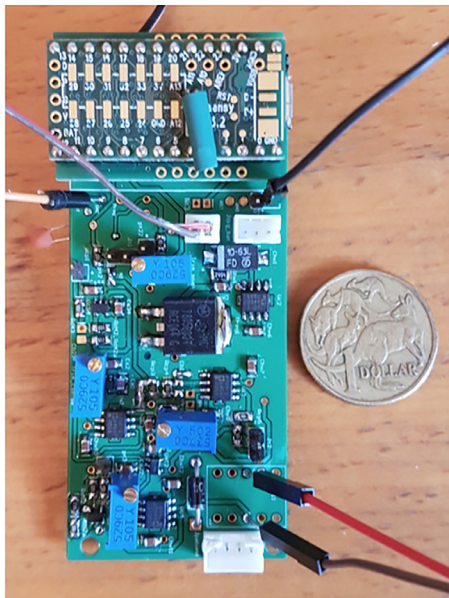
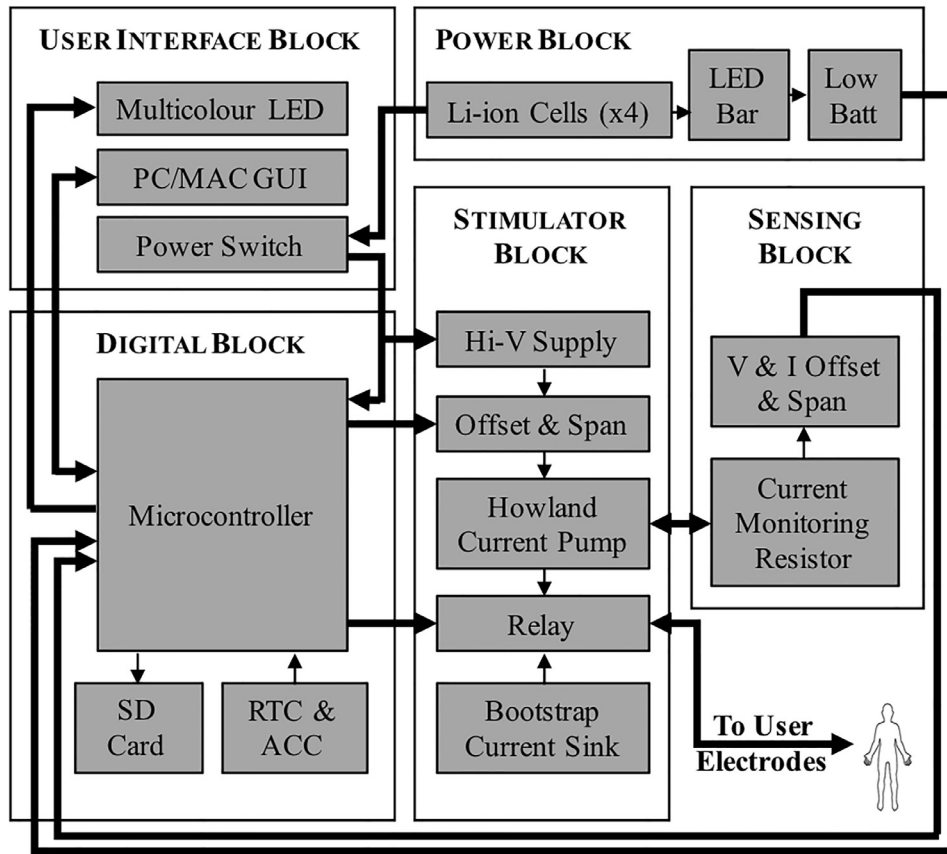


Fig. 1. Top: Stimulator system block diagram. Bottom Left: Stimulator circuit board with Teensy 3.2 mounted. Bottom Right: Final embodiment of the stimulator system.

With a stimulus control signal range of  $\pm 2.5\text{V}$ , to achieve the desired stimulus output of  $\pm 2.5\text{mA}$  the circuit was set for  $1\text{mA/V}$  voltage-to-current conversion (See supplementary material for details).

2.2.3. Relay

A double-pole, double-throw relay (Panasonic TQ2-5V-3) allows the stimulation electrodes to be connected/disconnected to the

stimulus load. The electrodes are connected to the normally-open side of the relay ensuring the user is disconnected to the stimulator on start-up. The normally-closed side of the relay is shorted, allowing the microcontroller to go through a series of safety checks at start-up and periodically if required. This is discussed in greater detail in the software section. In series with the relay are two sense resistors (RSENSE1 & RSENSE2) which are used for measurement of the voltage across and current through the relay.

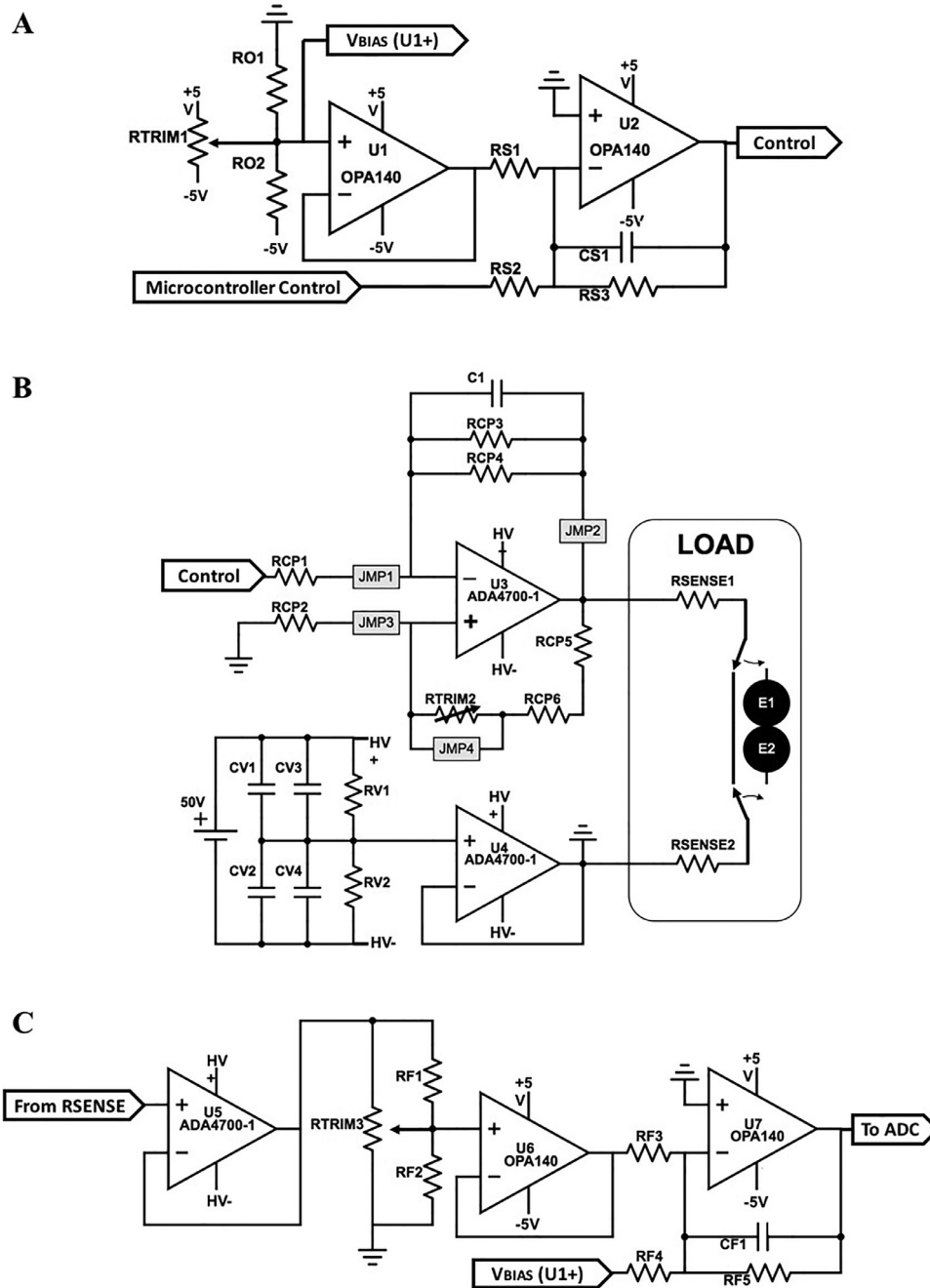


Fig. 2. (A) Offset and span circuit for the current pump input. (B) Modified Howland current pump circuit. (C) High-voltage compliant sensing circuit.

### 2.3. Sensing block

The stimulator operates as a closely monitored system to ensure the safety of the user and to ensure the desired stimulus is being applied appropriately. Detection of potentially harmful conditions, e.g. high electrode impedance, is performed by continuous monitoring of the stimulation voltage and current at ~100 Hz. This sensing system is also used during start-up to ensure the stimulator system is operating correctly and to check electrode impedance. Stimulation current and voltage drop across the stimulation electrodes are measured by dedicated high-voltage compliant circuitry (Fig. 2C).

### 2.4. Digital block

The microcontroller circuitry is responsible for generation of the arbitrary waveform, monitoring the applied voltage/current, system testing and error management. The system is implemented in firmware running on a small (18 × 36 × 6 mm) open-source embedded platform: Teensy 3.2 (PJRC, Sherwood, OR, USA). This microcontroller board was chosen primarily as it has 12-bit DAC and two concurrent 16-bit ADC's (13 usable bits). The core is a 72 MHz Cortex-M4, with 256 kB Flash Memory, 64 kB RAM and a 2 kB EEPROM. An internal real-time clock requires an external 32.768 kHz crystal and 3V coin battery. Programming and external

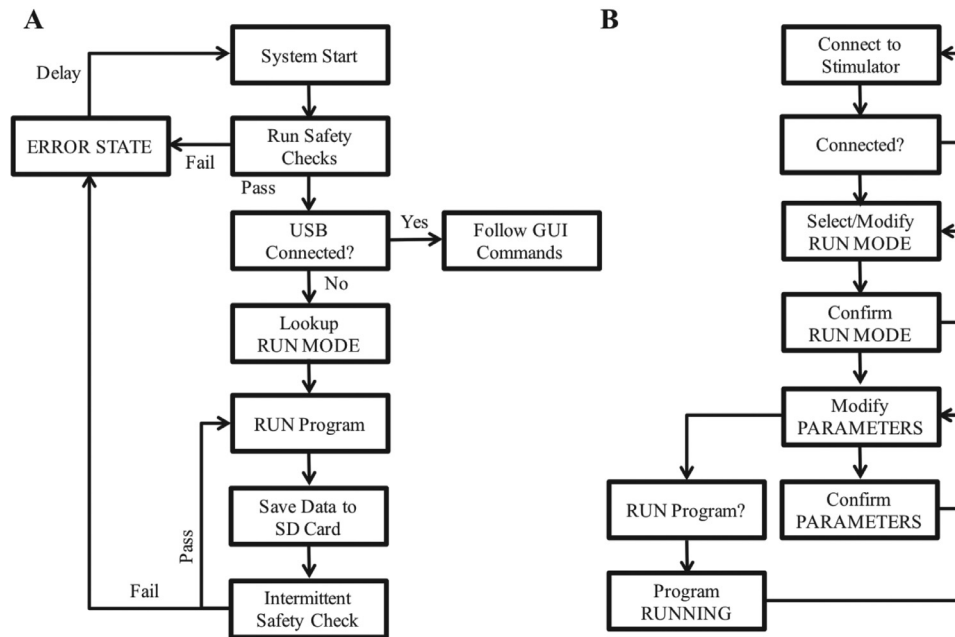


Fig. 3. System software flowcharts for (A) the microcontroller and (B) the graphical user interface.

communication is achieved via USB. Data is logged to an SD card using a convenient, pin-matched, SPI connected WIZ820\_SD\_Adapter (PJRC, Sherwood, OR, USA) without the optional ethernet socket, reducing the board space requirements. An MMA8415Q (NXP Semiconductors, Eindhoven, Netherlands) three axis 14-bit accelerometer is connected via an I2C port. Stimulator battery power is also constantly monitored by the microcontroller. A multicolour LED is used to communicate operational and error states to the user.

#### 2.4.1. Microcontroller software

The system firmware was designed such that it may operate either independently or under the control of an external computer running a graphical user interface and connected via USB. Four operation modes are implemented in this initial embodiment, however, many more can be easily implemented and added to the firmware and user interface. Fig. 3 provides a software flowchart emphasising how the embedded firmware and user interface interact.

The microcontroller software was developed in Arduino Software (version 1.6.9), an open source and highly supported programming language and embedded on Teensy 3.2 microcontroller boards as previously described. This embedded system was selected as it met both the requirements of the project and a preference to enable future open-source development of the stimulator.

**System start/safety checks:** The system starts with the output relay in the inactive state with the stimulation electrodes bypassed by the relay. The output current is also set to zero, providing double fault protection of the user from any transient outputs.

As the only indication of functionality is indicated by a three colour LED (red, green, blue), these colours are cycled through initially. The following series of safety checks are performed without the user connected – battery voltage level, zero current output, positive going current impedance and negative going current impedance. These safety checks are then repeated, but with the relay switched and the user connected via the electrodes. In all cases a very low level stimulus is used to perform the impedance check. Failure of any of these system checks results in an error state, soft shutdown of the system and the LED turning red, or blue if user impedance was at issue.

**Modes of operation:** The stimulator operates under its own automated control or, in the event that a USB connection is detected, under the control of the graphical user interface (GUI). Control of the stimulator via the GUI will be discussed in the *User Interface Block* section.

In the event that a USB connection is not detected, the microcontroller looks up user set system parameters (e.g. maximum stimulus amplitude) and RUN MODE to be employed. These parameters are saved in EEPROM memory. Four RUN MODES exist in the current system. Noise stimuli are based on prior art [12,28,29].

- Continuous Sine – A sinusoidal stimulus is applied via the electrodes at a user set amplitude and frequency.
- Continuous Noise – Pink noise is applied based on a user set amplitude.
- Threshold Sine – A sinusoidal is applied at 20/40/60/80/100% of a predefined maximum amplitude. Each is applied for a pre-set period of time (30 s).
- Threshold Noise – Pink noise is applied at 20/40/60/80/100% of a predefined maximum amplitude. Each is applied for a pre-set period of time (30 s).

The pre-set RUN MODE is then commenced and will operate continuously while simultaneously storing accelerometer signals, current applied and voltage applied data to an SD card and performing intermittent safety check (e.g., battery level and electrode impedance).

#### 2.5. User interface block

There are only three means of user communication with the device. A power switch, a single RGB LED and a graphical user interface (GUI) which allows setting of mode and output amplitude (Fig. 4, see supplementary material for GUI operation details)

### 3. Results

A variety of bench tests were performed on assembled prototype circuits. With the device set to generate a maximum current of 2.5 mA across a 10 k $\Omega$  load, the device consumes ~15 mA, as measured at the output of the high-voltage step-up circuit. The relatively high current consumption is largely due to the four

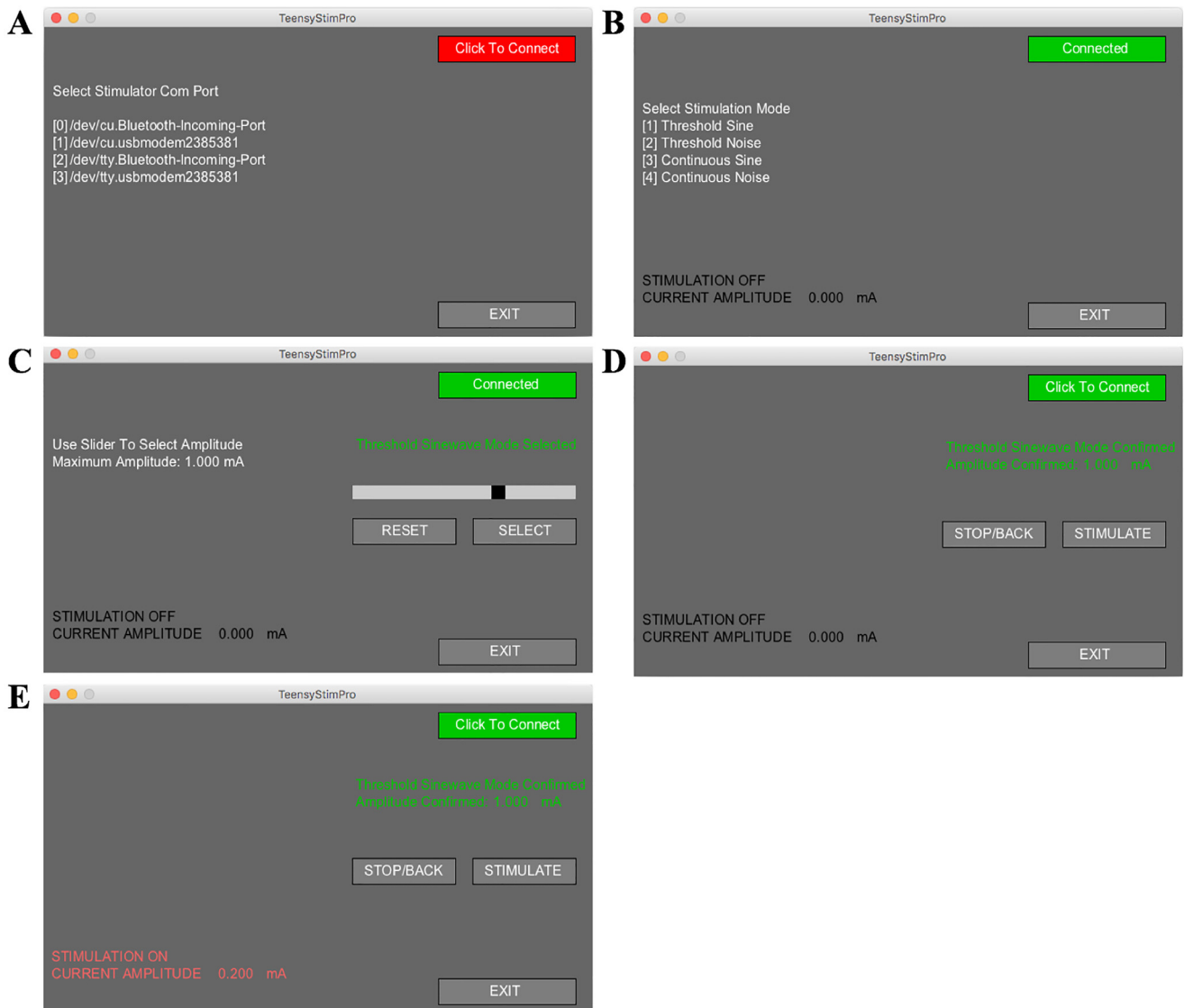


**Fig. 4.** Stimulator graphical user interface screenshots. Example use-case for application of threshold sinewave series of increasing amplitudes up to maximum of 1 mA. See text for details.

ADA4700-1 which, according to the technical documentation, typically require 1.7 mA quiescent current and by the dissipation of the two linear regulators (LM7805 and LM7905) required to generate the dual 5 V rail necessary for the driving/sensing circuitry.

As mentioned, the current source bandwidth is limited by the feedback capacitor C1. The addition of this capacitor is deemed necessary as the assembled prototype exhibits a natural low pass characteristic at  $\sim 750$  kHz. The current measured through the load decreases very rapidly to this frequency and then increase very rapidly from frequencies  $> 1$  MHz. Adding a 1 nF C1 capacitor increases the overall stability of the circuit and the current source has a flat bandwidth response up to 500 Hz to then reach a  $-3$  dB cut-off at  $\sim 2$  kHz. The magnitude response then continues to fall at  $-20$  dB per decade with a negligible amplitude at frequencies  $> 1$  MHz where the presence of instability was previously observed. None of the assembled prototypes after the addition of the stabilizing capacitor C1 showed instability.

The assembled circuit, behaves as a second order low-pass system with a cut-off frequency measured at 299 Hz (See supplementary material for bode plots).

The entire circuit except for the batteries and high-voltage supply is etched onto a four copper layers printed circuit board measuring  $87 \times 37$  [mm]. The two PCBs and the three batteries are arranged into a small prototype custom designed plastic box with external measurements of  $115 \times 55 \times 33$  [mm] which also provides direct access to the datalogging SD card and USB connection for programming/GUI control of the stimulator. The accompanying battery box measures  $115 \times 70 \times 31$  [mm]. Combined, with batteries inserted, they weigh 330 g. While a variety of electrodes and electrode cables could be used, we have chosen to use existing Alpha-Stim cables (Electromedical Products Int., Mineral Wells, TX, USA) for convenience. These are modified to add an inline 5 mA fast blow fuse as an additional safety measure (Model 273.005, Littelfuse, Inc., Chicago, IL, USA).

A demonstration of the functionality of the device as applied to a human subject is shown in Fig. 5. Voltage and current applied are shown as well as the impedance measured in 10 s windows. The application of a continuous sine wave is shown (Amplitude  $\pm 0.3$  mA, 0.1 Hz) followed by transition to continuous noise (Noise limits  $\pm 0.3$  mA).

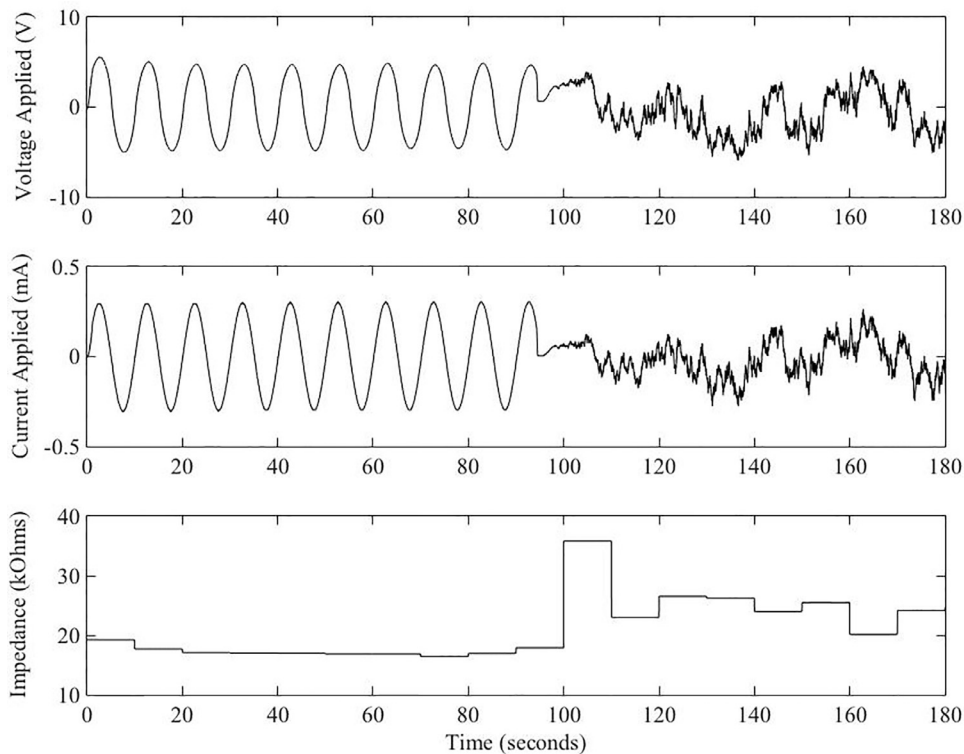


**Fig. 5.** Voltage (Top Panel) and current (Middle Panel) applied to healthy human subject with the application of a sinusoid and noise stimulus. Impedance is shown in 10 s windows.

Based on further testing, in operation with a sinewave applied at maximum output, the user can expect to achieve a minimum of 4 h' continuous use from a single battery pack.

#### 4. Discussion and Conclusion

Wearable arbitrary waveform constant current stimulators suitable for long-term use and clinical research are not currently available. Despite several potential applications of this type of technology for sensory enhancement/restoration it is difficult to explore potential real-world benefits of this new form of neuromodulation without the requisite technology. Considering the potential clinical applications alone (e.g., for neuropathy reversal, following nerve injury, falls prevention), making such devices available to physiologist and clinician could accelerate the development of a variety of new treatments.

This paper describes an effort to develop such a device. It is by no means perfect but is usable complete solution for clinical evaluation of a number of long-term applications of neural facilitation. It is intended to serve as a primer for anyone developing a similar solution and one that we anticipate will be surpassed in due course. We are aware of only one other design that provides for continuous (non-pulsatile) stochastic output with reasonably voltage and current compliance. The design by Yamamoto [19] has lower power requirements and a battery life of 24 h, considerably longer than our 4 h. This is likely due to our larger voltage ( $\pm 25$  V versus  $\pm 10$  V) and current ( $\pm 2.5$  mA versus  $\pm 1$  mA) compliance. We are in the process of developing a new stimulator system based on a novel bootstrapped current generator which promises up to  $\pm 72$  V compliance with much lower power consumption ( $< 300$  mW) [30]. Recommended areas of focus include improvement of power consumption, instrumentation and consolidation of power source to a single battery. Further benefits could be derived

from taking advantage of wireless communication, smart phone technology and potentially cloud based computing.

The developed stimulator platform is sufficient for long-term clinical trials of any previously mentioned laboratory based experiments cohorts [8–13]. Advancement of the technology will continue in parallel with planned clinical trials.

#### Acknowledgements

The authors would like to thank Colin Symons and Andrew Nicolson for their help in building the device.

#### Competing interests

None declared.

#### Funding

This work was supported by the National Health and Medicine Research Council NHRMC (grant APP1067353) and USAMRAA (grant W81XWH-14-2-0012).

#### Ethical approval

Rutgers Institutional Review Board (Pro20170001287).

#### Supplementary material

Supplementary material associated with this article can be found, in the online version, at doi:10.1016/j.medengphy.2019.04.001.

## References

- [1] Shaumburg H, Spencer P, Ochoa J. The aging human peripheral nervous system. Davis: Philadelphia; 1983.
- [2] Jordan B, Cummings J. Mental status and neurologic examination in the elderly. Principles of Geriatric Medicine and Gerontology. Ettinger W, editor. New York: McGraw-Hill; 1999.
- [3] Patel S, Hyer S, Tweed K, Kerry S, Allan K, Rodin A, et al. Risk factors for fractures and falls in older women with type 2 diabetes mellitus. *Calcif Tissue Int* 2008;82:87–91. doi:10.1007/s00223-007-9082-5.
- [4] Levin M. Pathogenesis and general management of foot lesions in the diabetic patient. In: Bowkers J, Pfeifer M. *The Diabetic Foot*. 6th ed., 2001, p. 222.
- [5] Allan LM, Ballard CG, Rowan EN, Kenny RA, Ferri C, Prince M, et al. Incidence and prediction of falls in dementia: a prospective study in older people. *PLoS One* 2009;4:e5521. doi:10.1371/journal.pone.0005521.
- [6] Tinetti ME, Liu WL, Claus EB. Predictors and prognosis of inability to get up after falls among elderly persons. *JAMA* 1993;269:65–70.
- [7] McDonnell MD, Ward LM. The benefits of noise in neural systems: bridging theory and experiment. *Nat Rev Neurosci* 2011;12:415–26. doi:10.1038/nrn3061.
- [8] Priplata Aa, Niemi JB, Salen M, Harry JD, Lipsitz La, Collins JJ. Noise-enhanced human balance control. *Phys Rev Lett* 2002;89:238101. doi:10.1103/PhysRevLett.89.238101.
- [9] Gravelle DC, Laughton CA, Dhruv NT, Katdare KD, Niemi JB, Lipsitz LA, et al. Noise-enhanced balance control in older adults. *Neuroreport* 2002;13:1853–6.
- [10] Priplata AA, Patriitti BL, Niemi JB, Hughes R, Gravelle DC, Lipsitz LA, et al. Noise-enhanced balance control in patients with diabetes and patients with stroke. *Ann Neurol* 2006;59:4–12. doi:10.1002/ana.20670.
- [11] Ming-Yih L, Chin Feng L, Kok Soon S. New foot pressure activated sensory compensation system for posture-control enhancement in amputees. *IEEE/ASME Trans Mechatron* 2007;12:236–43.
- [12] Breen PP, ÓLaighin G, McIntosh C, Dinneen SF, Quinlan LR, Serrador JM. A new paradigm of electrical stimulation to enhance sensory neural function. *Med Eng Phys* 2014;36:1088–91. doi:10.1016/j.medengphy.2014.04.010.
- [13] Breen PP, Serrador JM, O'Tuathail C, Quinlan LR, McIntosh C, ÓLaighin G. Peripheral tactile sensory perception of older adults improved using subsensory electrical noise stimulation. *Med Eng Phys* 2016;38:822–5. doi:10.1016/j.medengphy.2016.05.015.
- [14] Akay M, editor. *Wiley encyclopedia of biomedical engineering*. John Wiley & Sons, Ltd; 2006.
- [15] Webster J.G. *Medical instrumentation application and design*, 4th ed. John Wiley & Sons, Ltd.
- [16] Assambo C, Burke MJ. Low-frequency response and the skin-electrode interface in dry-electrode electrocardiography. *Advances in Electrocardiograms - Methods and Analysis*. Millis R, editor. InTech; 2012. doi:10.5772/22777.
- [17] Breen PP, Corley GJ, O'Keefe DT, Conway R, ÓLaighin G. A programmable and portable NMES device for drop foot correction and blood flow assist applications. *Med Eng Phys* 2009;31:400–8.
- [18] Valtin M, Kociemba K, Behling C, Kuberski B, Becker S, Schauer T. RehaMove-Pro: a versatile mobile stimulation system for transcutaneous FES applications. *Eur J Transl Myol* 2016;26:6076. doi:10.4081/ejtm.2016.6076.
- [19] Yamamoto Y, Struzik ZR, Soma R, Ohashi K, Kwak S. Noisy vestibular stimulation improves autonomic and motor responsiveness in central neurodegenerative disorders. *Ann Neurol* 2005;58:175–81. doi:10.1002/ana.20574.
- [20] Breen PP, Macefield VG. Proximally applied subsensory electrical noise stimulation reduces variance in action potential timing and enhances sensory perception. In: Proceedings of the IEEE/EMBS conference on neural engineering. IEEE; 2013. p. 267–70. doi:10.1109/NER.2013.6695923.
- [21] Burr-Brown. OPA244 MicroPower, Single-Supply OPERATIONAL AMPLIFIERS MicroAmplifier TM Series. 2008.
- [22] Texas Instruments. LM2587 SIMPLE SWITCHER® 5A Flyback Regulator. 2013.
- [23] Breen PP, Serrador JM, O'Tuathail C, Quinlan LR, McIntosh C, ÓLaighin G. Peripheral tactile sensory perception of older adults improved using subsensory electrical noise stimulation. *Med Eng Phys* 2016;38. doi:10.1016/j.medengphy.2016.05.015.
- [24] Serrador JM, Deegan BM, Geraghty MC, Wood SJ. Enhancing vestibular function in the elderly with imperceptible electrical stimulation. *Sci Rep* 2018;8:336. doi:10.1038/s41598-017-18653-8.
- [25] Dhruv NT, Niemi JB, Harry JD, Lipsitz La, Collins JJ. Enhancing tactile sensation in older adults with electrical noise stimulation. *Neuroreport* 2002;13:597–600. doi:10.1097/00001756-200204160-00012.
- [26] Horowitz P, Hill W. *The art of electronics*. Third ed. Cambridge; 2015.
- [27] Analog Devices. ADA4700-1 high voltage, precision operational amplifier. 2013.
- [28] Pavlik AE, Inglis JT, Lauk M, Oddsson L, Collins JJ. The effects of stochastic galvanic vestibular stimulation on human postural sway. *Exper Brain Res* 1999;124:273–80.
- [29] Breen PP, Macefield VG. Proximally applied subsensory electrical noise stimulation reduces variance in action potential timing and enhances sensory perception. In: Proceedings of the 2013 6th International IEEE/EMBS conference on neural engineering. IEEE; 2013. p. 267–70. doi:10.1109/NER.2013.6695923.
- [30] Karpul D, Cohen GK, Gargiulo GD, Schaik A, McIntyre S, Breen PP. Low-power transcutaneous current stimulator for wearable applications. *Biomed Eng Online* 2017;16. doi:10.1186/s12938-017-0409-9.